

# Dynamic analysis of spur gears considering centrifugal stiffness and geometric eccentricity

Zhuangzhuang Zhang <sup>a</sup>, Fuhao Liu

School of Mechanical and Automotive Qingdao University of Technology, Qingdao 266520, China.

<sup>a</sup>1079527468@qq.com

## Abstract

Gear systems inevitably suffer from geometric eccentricity errors that result in the center of mass and center of rotation not coinciding. During the gear meshing process, the gear center distance and the gear tooth meshing condition change with time. In this paper, a model considering geometric eccentricity is proposed and the effect of centrifugal stiffness is taken into account. Finally, the dynamic response under different eccentricity and initial eccentricity angle is discussed.

## Keywords

Geometric eccentricity, centrifugal stiffness, eccentricity, initial eccentricity angle, dynamic response.

## 1. Introduction

With the wide application of gear systems in industry, the dynamic response analysis of gear systems becomes particularly important in improving the stability of the system and reducing the vibration noise of the system. Therefore, it is necessary to establish a more realistic dynamic model.

Calculation of gear meshing stiffness is an important research topic as it plays a crucial role in gear dynamics [1, 2, 3]. Therefore, accurate assessment of meshing stiffness helps to reliably predict high-speed gear dynamics and optimize the design.

In addition, the eccentricity due to manufacturing and assembly errors, such as runout errors, its will inevitably appear in actual gear systems. phadatare h p et al [4] analyzed the effect of mass eccentricity on lightweight flexible rotor-disk-rotor systems. zhao bai-shun et al [5] proposed a method for loaded gear tooth contact with improved eccentricity, and verified it. yuan bing et al [6] analyzed the quasi-static characteristics of helical gear system containing manufacturing error and runout error. In the previous studies [7, 8, 9], some scholars investigated the effect of eccentricity on the dynamic characteristics of the gear system; however, the effect of the initial phase on the dynamic response of the gear system was not analyzed in detail.

In the above studies, scholars have not considered the effect of the coupling of centrifugal stiffness and eccentricity on the gear system. Therefore, it is necessary to analyze the effect of geometric eccentricity on the gear system when studying centrifugal stiffness. The author establishes a dynamic model of a two-degree-of-freedom spur gear system containing geometric eccentricity, and analyzes the effects on the system at different eccentricity distances and different initial eccentricity angles.

## 2. Spur gear system dynamics modeling

### 2.1 Definition of parameters of spur gear system with geometric eccentricity faults

Table 1 Gear pairs data.

| Parameter                             | Pinion/Gear |
|---------------------------------------|-------------|
| Number of teeth                       | 27/36       |
| Tooth width (mm)                      | 10          |
| Module (mm)                           | 2.5         |
| Modulus of elasticity (G·Pa)          | 207         |
| Initial pressure angle $\alpha_0$ (°) | 20          |
| Mesh damping ratio $\xi_m$            | 0.25        |
| Backlash(m)                           | 1E-4        |

### 2.2 Dynamic model with geometric eccentricity

Fig. 1 illustrates a 2-dof parametric model of a pair of involute spur gear trains considering geometric eccentricity. In this model, the shaft, pinion and large gears are defined as rigid except for the teeth. The geometrical eccentricities of the pinion and the large mobile gear are  $\rho_p$  and  $\rho_g$ , respectively; the angular vibrations of the pinion and the large gear are  $\theta_p$  and  $\theta_g$ , respectively;  $O_p$ , and  $O_g$  are the centers of circles of the pinion and the large gear, respectively;  $G_p$  and  $G_g$  are the centers of rotation of the driving gear and the driven gear, respectively;  $m_i$  is the mass of the gear  $i$  ( $i = p, g$ );  $J_i$  is the moment of inertia of the gear  $i$  relative to the center of rotation;  $\omega_i$  is the nominal angular velocity of gear  $i$ ;  $T_i$  is the torsional torque applied to gear  $i$ .

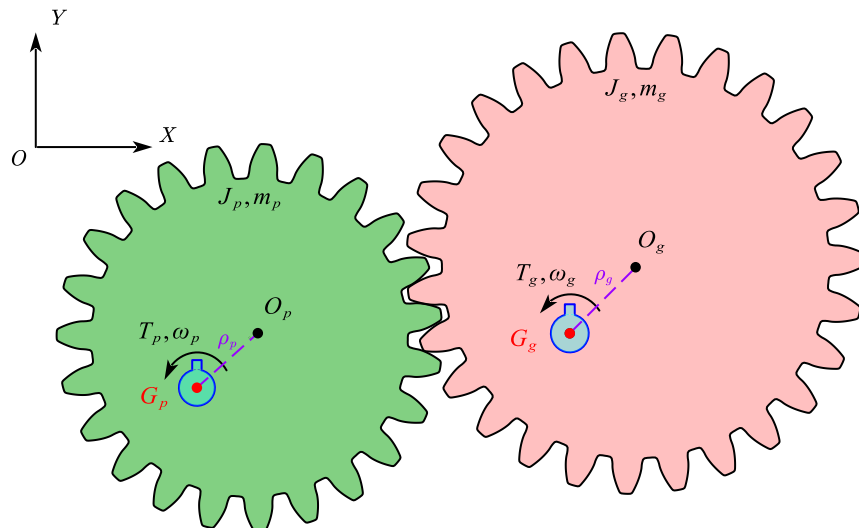


Fig. 1 Parametric Modeling of Spur Gear Units with Geometric Eccentricity

When gears are geometrically eccentric, the geometric eccentricity error will affect the gear system and be reflected in the centrifugal and inertial forces [10].

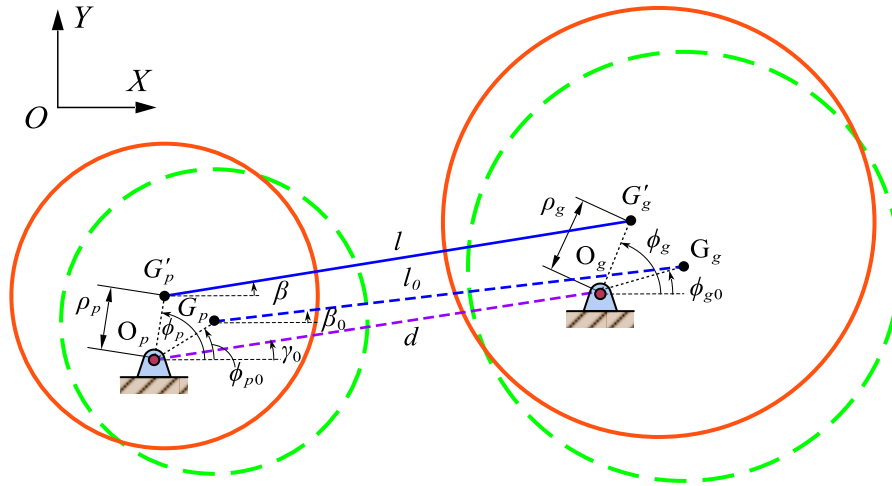


Fig. 2 Generalized coordinates for the gear pair

Fig. 2 describes the generalized coordinates for the mated gear pair. The motion of the gear set is rotary. The dashed and solid circles represent the gear pair before and after motion, respectively. Due to the presence of geometric eccentricity the initial center distance is  $d_0$ .  $\gamma_0$  and  $\gamma$  are the initial and actual mounting angles of the large gear in relation to the pinion gear, respectively. Here, two static coordinate systems  $O_i x_i y_i$  ( $i = p, g$ ) are established on the axis centers  $O_p$  and  $O_g$ , respectively. The angle  $\beta$  represents the position of the gear relative to the pinion after motion.  $d$  is the actual center distance,  $l$  is the distance between the two centers of mass  $G'_p$  and  $G'_g$  after the motion of the gear pair.  $\phi_{p0}$  and  $\phi_{g0}$  are the initial eccentricity angles. The rotation angle displacements of gear  $i$  are given by angular coordinates,  $\phi_p$  and  $\phi_g$ , which can be expressed as follows:

$$\phi_p(t) = \theta_p + \phi_{p0}, \phi_g(t) = \theta_g + \phi_{g0} \tag{1}$$

where  $\theta_i$  is the torsional angle displacement superimposed on the rigid-body rotation of gear  $i$ . The relationship between the coordinates of the center point and the center of rotation can be found from geometric relationships.

$$X_{G_p} = \rho_p \cos(\phi_{p0}), Y_{G_p} = \rho_p \sin(\phi_{p0}) \tag{2}$$

$$X_{G_g} = \rho_g \cos(\phi_{g0}), Y_{G_g} = \rho_g \sin(\phi_{g0}) \tag{3}$$

$$X_{G'_p} = \rho_p \cos(\phi_p), Y_{G'_p} = \rho_p \sin(\phi_p) \tag{4}$$

$$X_{G'_g} = \rho_g \cos(\phi_g), Y_{G'_g} = \rho_g \sin(\phi_g) \tag{5}$$

$l_0$  is the distance between  $G_p$  and  $G_g$ . which can be expressed as:

$$l_0 = R_{bp} + R_{bg} \tag{6}$$

where  $R_{bi}$  is the radius of the base circle of gear  $i$ . The actual center distance  $d$  is given by

$$d = d_0 = \sqrt{(X_{G_p} - X_{G_g} + l_0 \cos(\beta_0))^2 + (Y_{G_p} - Y_{G_g} + l_0 \sin(\beta_0))^2} \tag{7}$$

The distance  $l$  between two centers of mass can be expressed as:

$$l = \sqrt{(X_{G'_g} - X_{G'_p} + d_0 \cos(\gamma_0))^2 + (Y_{G'_g} - Y_{G'_p} + d_0 \sin(\gamma_0))^2} \tag{8}$$

The position angle  $\beta$  can be expressed as:

$$\beta = \tan^{-1} \frac{Y_{G'_g} - Y_{G'_p} + d_0 \sin(\gamma_0)}{X_{G'_g} - X_{G'_p} + d_0 \cos(\gamma_0)} \tag{9}$$

$\gamma$  is the angle between  $d$  and the positive semi-axis of  $x$ .

$$\cos(\gamma) = \frac{d_0 \cos(\gamma_0)}{d}, \sin(\gamma) = \frac{d_0 \sin(\gamma_0)}{d} \quad (10)$$

According to the gear mesh relationship, the dte (dynamic transmission error) between two mating gears along the loa which can be written as:

$$\delta_L = R_{bp}\psi_p + R_{bg}\psi_g \quad (11)$$

In order to ensure the formation of normal lubricating oil film between tooth surfaces and prevent gear teeth from getting stuck due to thermal expansion deformation caused by the increase of gear operating temperature, an appropriate gear backlash should be considered. According to ref. [11], dynamic half backlash due to dynamic changing of axle center distance can be derived as:

$$b_t(t) = b_0 + (l - l_0)\tan(\alpha) \quad (12)$$

$\dot{\delta}(t)$  and  $\dot{b}_t(t)$  are the derivatives of  $\delta(t)$  and  $b_t(t)$  respectively, which can be calculated as:

$$\dot{\delta}_L(t) = \delta_{L,\theta_p}\dot{\theta}_p + \delta_{L,\theta_g}\dot{\theta}_g \quad (13)$$

$$\dot{b}_t(t) = b_{t,\theta_p}\dot{\theta}_p + b_{t,\theta_g}\dot{\theta}_g \quad (14)$$

where  $\delta_{L,\theta_p}$  is the deflection of dte with respect to torsional direction,  $b_{t,\theta_p}$  is the deflection of the tooth gap with respect to the torsional direction, which can be calculated as:

$$\delta_{L,\theta_p} = \rho_p \cos(\phi_p + \varphi) - \frac{\rho_p \left( (R_{bp} + R_{bg}) \cos(\alpha) \sin(\phi_p - \beta) \right)}{l \sin(\alpha)} + R_{bp} \quad (15)$$

$$\delta_{L,\theta_g} = -\rho_g \cos(\phi_g + \varphi) + \frac{\rho_g \left( (R_{bp} + R_{bg}) \cos(\alpha) \sin(\phi_g - \beta) \right)}{l \sin(\alpha)} + R_{bg} \quad (16)$$

$$b_{t,\theta_p} = \rho_p \sin(\alpha) \sin(\phi_p - \beta) \quad (17)$$

$$b_{t,\theta_g} = -\rho_g \sin(\alpha) \sin(\phi_g - \beta) \quad (18)$$

The equation of motion of the system is:

$$(I_p + m_p \rho_p^2) \ddot{\theta}_p + \sum_{\tau=1}^n T_{m_p}^\tau = T_p \quad (19)$$

$$(I_g + m_g \rho_g^2) \ddot{\theta}_g + \sum_{\tau=1}^n T_{m_g}^\tau = T_g \quad (20)$$

where  $\tau$  is the number of contact teeth at any given moment.

$T_{m_p}$  and  $T_{m_g}$  are the dynamic mesh torque of the gear after considered the mesh stiffness which is related to  $\theta$ , respectively. And can be calculated as:

$$T_{m_{p,g}}^\tau = \delta_{L,\theta_{p,g}} \left( k_m^\tau f(\delta_L, b_t) + c_m^\tau f_1(\delta_L, b_t) \right) \quad (21)$$

$f(\delta, b_t)$  is the nonlinear functions for backlash, which can be expressed as [12]:

$$f(\delta_L, b_t) = \begin{cases} \delta_L(t) - \text{sign}(\delta_L) b_t & |\delta_L| \geq b_t \\ 0 & |\delta_L| < b_t \end{cases} \quad (22)$$

$$f_1(\delta_L, b_t) = \begin{cases} \dot{\delta}_L(t) - \text{sign}(\delta_L) \dot{b}_t & |\delta_L| \geq b_t \\ 0 & |\delta_L| < b_t \end{cases} \quad (23)$$

### 3. Centrifugal Rigidity

We control the stiffness of the t-to-meshing gear by angular velocity expressed in  $k_m^\tau$ , then during the grid period,  $k_m^\tau$  is expressed as:

$$k_m^1(\dot{\theta}_p, \dot{\theta}_g) = \frac{1}{1/k_p^{n_j}(\dot{\theta}_p) + 1/k_g^{n_j}(\dot{\theta}_g) + 1/k_h} \tag{24}$$

$$k_m^2(\dot{\theta}_p, \dot{\theta}_g) = \begin{cases} \frac{1}{1/k_p^{n_n - n_v + n_j}(\dot{\theta}_p) + 1/k_g^{n_n - n_v + n_j}(\dot{\theta}_g) + 1/k_h} & 1 \leq n_j \leq n_v \\ 0 & n_v < n_j \leq n_n - n_v + 1 \end{cases} \tag{25}$$

here  $k_{p,g}^i$  denote the mesh stiffness for the  $i$  mesh point on pinion and gear in one mesh period; the  $k_h$  is the Hertz stiffness.

The comprehensive meshing stiffness  $k_{md}$  of the two-tooth meshing is

$$k_{md}(\dot{\theta}_p, \dot{\theta}_g) = k_m^1(\dot{\theta}_p, \dot{\theta}_g) + k_m^2(\dot{\theta}_p, \dot{\theta}_g) \tag{26}$$

### 4. Centrifugal stiffness and dynamics analysis

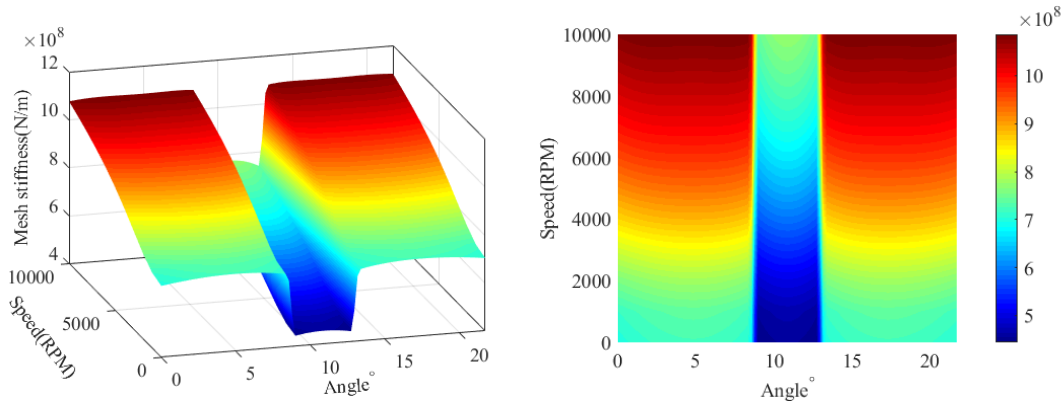


Fig. 3 Combined centrifugal stiffness

Fig. 3 shows a three-dimensional plot of the meshing stiffness of the gear pair (0 to 10000 r/min) at different speeds. At higher speeds, the centrifugal effect of the gear pair is evident and the centrifugal stiffness is proportional to the speed.

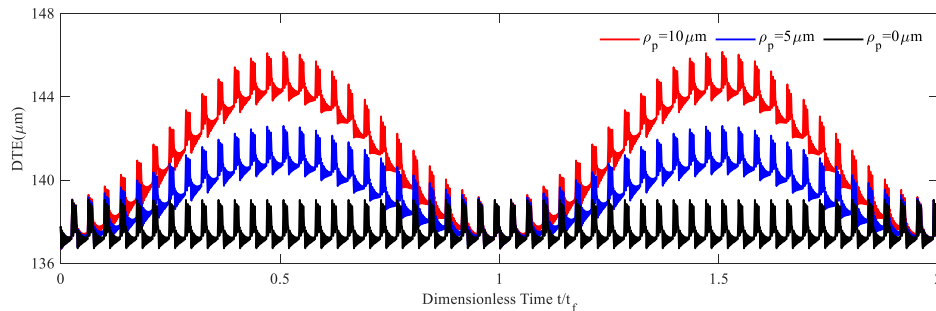


Fig. 4 Dynamic response at different eccentricity

The above figure shows the time-domain diagram of dte with different eccentricity, from which it can be seen that the dte with eccentricity faults fluctuates periodically for one rotation period and the degree of fluctuation becomes more and more drastic with the increase of eccentricity.

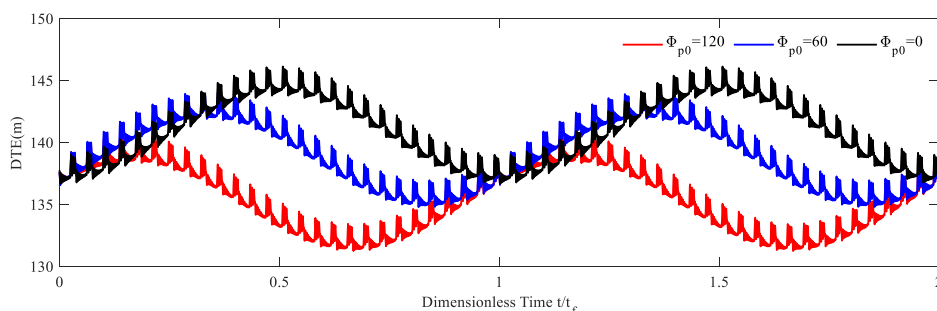


Fig. 5 Dynamic response at different initial eccentricity call angles

The upper figure shows the time-domain plot of the dte at different initial eccentricity angles, from which it can be seen that the amplitude and phase of the dte change as the initial eccentricity angle increases.

In order to observe more clearly the changes in the peak value and phase of the dte, the following figure shows the envelope of the peak value on the dte.

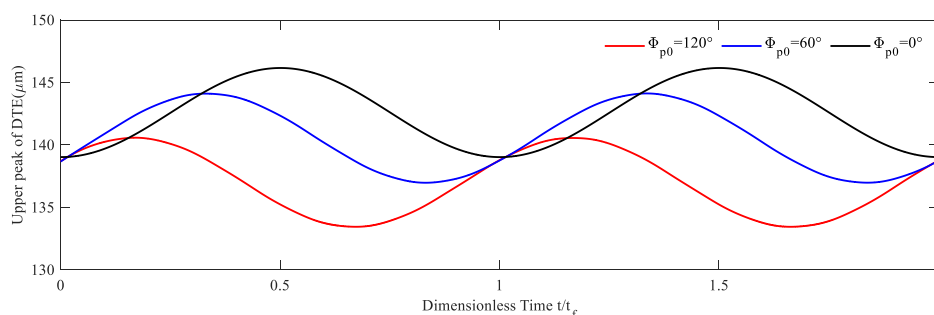


Fig. 6 Envelopes for different initial eccentricity call angles

Fig. 7 shows the frequency sweep of the initial eccentricity angle at different eccentricity rates, the initial eccentricity angle is fluctuating sinusoidally with 360° as a fluctuation period, and the larger the eccentricity rate the larger the image fluctuation. When the initial eccentricity angle is 180°, the dte is minimized at this time, when the eccentricity rate is certain, the reasonable placement of the eccentric gear can largely reduce the eccentricity fault on the dynamic response of the system, when the initial eccentricity angle of the eccentric gear is 180°, the impact is minimized

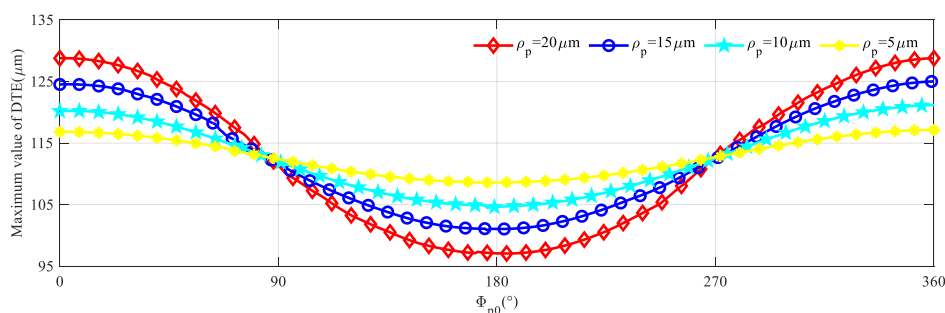


Fig. 7 Frequency sweeps for initial eccentricity angles at different eccentricity rates

### 5. Conclusion

The centrifugal stiffness becomes larger as the rotational speed increases, and the presence of eccentricity causes periodic fluctuations in the dte, whose period of fluctuation is the rotation period. Reasonable placement of the gear pair can reduce the vibration response of the gear pair and improve the stability of the system, when the difference in the initial eccentricity angle of the large and small gears is 180°.

## References

- [1] del Rincon, A.F., et al., A model for the study of meshing stiffness in spur gear transmissions. *Mechanism and Machine Theory*, 2013. 61: p. 30-58.
- [2] Khabou, M.T., et al., Study of a spur gear dynamic behavior in transient regime. *Mechanical Systems and Signal Processing*, 2011. 25(8): p. 3089-3101.
- [3] Liu, F.H., et al., Dynamic behavior analysis of spur gears with constant & variable excitations considering sliding friction influence. *Journal of Mechanical Science and Technology*, 2016. 30(12): p. 5363-5370.
- [4] PHADATARE H P, PRATIHER B. Nonlinear modeling, dynamics, and chaos in a large deflection model of a rotor-disk-bearing system under geometric eccentricity and mass unbalance[J]. *Acta Mechanica*,2020,231(3):907-928.
- [5] ZHAO Bai-shun, HUANGFU Yi-fan, MA Hui, et al. The influence of the geometric eccentricity on the dynamic behaviors of helical gear systems[J]. *Engineering Failure Analysis*,2020,118 (1) : 104907.
- [6] YUAN Bing, CHANG Shan, LIU Geng, et al. Quasi-static and dynamic behaviors of helical gear system with manufacturing errors[J]. *Chinese Journal of Mechanical Engineering*,2018, 31(1): 1-9.
- [7] Zhao W.Q., Liu J., Zhao W.H., et al. An investigation on vibration features of a gear-bearing system involved pitting faults considering effect of eccentricity and friction[J]. *Engineering Failure Analysis*. 2022; 131.
- [8] Tian G., Gao Z.H., Liu P., et al. Dynamic Modeling and Stability Analysis for a Spur Gear System Considering Gear Backlash and Bearing Clearance[J]. *Machines*. 2022; 10(6).
- [9] Jiang H.J., Liu F.H. Dynamic modeling and analysis of spur gears considering friction-vibration interactions[J]. *Journal of the Brazilian Society of Mechanical Sciences and Engineering*. 2017; 39(12): 4911-4920.
- [10] Xiang L., Gao N. Coupled torsion-bending dynamic analysis of gear-rotor-bearing system with eccentricity fluctuation[J]. *Applied Mathematical Modelling*. 2017; 50: 569-584.
- [11] Li F.J., Li X.P., Qu X.C., et al. Nonlinear characteristic analysis of shaft-bearing-pedestal system considering damage of cylindrical roller bearing[J]. *International Journal of Non-Linear Mechanics*. 2023; 150.
- [12] Xu M.M., Han Y.Y., Sun X.Q., et al. Vibration characteristics and condition monitoring of internal radial clearance within a ball bearing in a gear-shaft-bearing system[J]. *Mechanical Systems and Signal Processing*. 2022; 165.